Uniform semiclassical and quantum calculations of Regge pole positions and residues for complex optical nuclear heavy-ion potentials

J. N. L. Connor
Department of Chemistry, University of Manchester, Manchester M13 9PL, United Kingdom

D. Farrelly
Department of Chemistry, University of Manchester, Manchester M13 9PL, United Kingdom
*and Department of Chemistry and Biochemistry, Utah State University, Logan, Utah 84322**
(Received 19 May 1993)

The first uniform semiclassical (SC) calculations of Regge pole positions and residues have been carried out for four complex optical potentials, which have been used to fit $^{16}O+^{28}Si$ elastic-scattering data at $E_{lab}=55$ MeV. In particular, we have extended a SC formalism developed for atomic and molecular scatterings to allow for the presence of a long-range Coulomb potential. The SC Regge poles and residues are compared with quantum results of Takemasa and Tamura [Phys. Rev. C **18**, 1282 (1978)], who numerically integrated the radial Schrödinger equation. The SC computations show that Takemasa and Tamura missed ten poles. Using a modified version of the quantum computer code REGGE, due to Takemasa, Tamura, and Wolter [Comput. Phys. Commun. **18**, 427 (1979)] we have located five of these poles—the remaining poles have residues of modulus $<10^{-8}$. For low values of the Regge pole quantum number n, the SC and quantum pole positions are in close agreement, with larger differences for the residues. As n increases, the SC results become less accurate. However at high values of n, the quantum results also lose accuracy due to numerical instabilities in the REGGE code. It is demonstrated that the choice of Coulomb interaction—charged sphere or pure Coulomb—can significantly effect the properties of the Regge pole positions and residues.

PACS number(s): 03.65.Sq, 12.40.Gg, 24.10.Ht, 25.70.Bc

I. INTRODUCTION

A powerful technique for understanding elastic angular scattering is the Regge pole formalism [1]. In this technique, the properties of the Regge pole positions and residues in the complex angular momentum plane play a fundamental role [2,3]. The development of efficient and accurate methods to calculate Regge pole positions and residues is thus an important problem.

Complex angular momentum techniques have been used to describe both nuclear heavy-ion and molecular collisions, which share the common property of being short-wavelength (or high-frequency) scattering phenomena [4,5]. The most popular approach for heavy-ion scattering has been to adopt a simple parametrized form for the scattering matrix element. This has the advantage that explicit formulas can often be assumed or deduced for the Regge pole positions and residues; see, e.g., Refs. [6–16]. A second approach is to start with an interaction potential function, for which the pole positions and residues are then calculated. This second approach has only been used a few times for heavy-ion collisions [17–22], with the most extensive quantum results being reported by Takemasa and Tamura (TT) [18].

In molecular scattering, the situation just described is reversed: Although simple parametrized scattering matrix elements have been used [23,24], the more popular approach has been to calculate the Regge pole positions and residues from an assumed potential [25–34]. In particular, uniform semiclassical (SC) techniques have been shown to yield accurate pole positions and residues. For reviews of complex angular momentum techniques as applied to molecular scattering, we refer to Refs. [35–38].

The purpose of this paper is to apply the SC techniques developed for molecular problems to nuclear heavy-ion scattering. We have used the same potentials as TT, so we can compare with their quantum results for the Regge pole positions and residues. The potentials are denoted SD, GK, E18, and LC, and have been used to fit $^{16}O+^{28}Si$ elastic-scattering data at $E_{lab}=55$ MeV [18]. They are described in Sec. II.

The SC theory is presented in Sec. III, where uniformly valid formulas for the pole positions and residues are derived. An important difference between nuclear heavy-ion and molecular scattering in the presence of a long range Coulomb tail for heavy-ion collisions. We show how to extend the SC theory of Ref. [26] to include this effect.

Our initial SC calculations revealed that TT failed to locate ten poles in a specified region of the first quadrant of the complex angular momentum plane. We therefore obtained the source code of the REGGE computer program they used [19] and with a modified version of it were able to find five of the missing poles, using the SC

*Present address.

pole positions as initial estimates. Section IV describes some practical points associated with the quantum and SC computations.

Our SC results for the Regge pole positions and residues are presented in Sec. V, where they are compared with the quantum values of TT together with our results from the REGGE code. We also investigate the effect of replacing a uniformly charged sphere potential (as used by TT) by a pure Coulomb potential. Our conclusions are in Sec. VI.

II. THE POTENTIALS

Takemasa and Tamura [18] have calculated quantum pole positions and residues for four complex optical nuclear potentials, three of which have the Woods-Saxon form,

$$V_N(r)=-\frac{V_0}{1+\exp[(r-R_1)/a_1]}-\frac{iW_0}{1+\exp[(r-R_2)/a_2]}\ , \tag{2.1}$$

where V_0 and W_0 are the strengths of the real and imaginary parts of the potential, respectively. The parameters for these potentials are given in Table I and correspond to the potentials of Shkolnik and Dehnhard (SD) [39], Golin and Kahana (GK) [40], and the E18 potential of Cramer *et al.* [41]. The fourth potential, due to Lee and Chan (LC) [42], has the modified form

$$V_N(r)=\frac{-(V_0+iW_0)}{1+0.99\exp[(r-R_1)/a_1]+\exp[(r-R_2)/a_2]}\ . \tag{2.2}$$

The parameters for this potential are also given in Table I. Three of these potentials have been found to reproduce the experimental elastic differential cross section for $^{16}O+^{28}Si$ reasonably well, although we shall not be concerned with this point.

In addition to the nuclear potential, it is also necessary to specify a Coulomb interaction. We follow Takemasa, Tamura, and Wolter [19] and use a uniformly charged sphere potential of radius R_C,

$$V_C(r)=\begin{cases}\dfrac{e^2Z_1Z_2}{r}\ , & r>R_C\ ,\\ \dfrac{e^2Z_1Z_2}{2R_C}\left[3-\left[\dfrac{r}{R_C}\right]^2\right]\ , & r\le R_C\ ,\end{cases} \tag{2.3}$$

where Z_1 and Z_2 are the atomic numbers of the colliding ions. Note that the parameters R_1, R_2, and R_C are related to r_1, r_2, and r_C in Table I by

$$R_i=r_i(A_1^{1/3}+A_2^{1/3})\ ,\quad i=1,2,C\ ,$$

where A_1 and A_2 are the relative atomic masses of the colliding ions. We will also report Regge pole calculations in Sec. V C using just a pure Coulomb potential for all r.

It is easy to see from Eq. (2.1) that the SD, GK, and E18 potentials each possess in the complex r plane an infinite number of poles that arise from the real and imaginary parts of the potential. The positions of these poles are

$$\begin{aligned} r_{V_0}^{(n)}&=R_1\pm i(2n+1)\pi a_1\ ,\quad n=0,1,2,\ldots,\\ r_{W_0}^{(m)}&=R_2\pm i(2m+1)\pi a_2\ ,\quad m=0,1,2,\ldots\ . \end{aligned} \tag{2.4}$$

The LC potential also has an infinite number of poles in the complex r plane, but in this case the positions of the poles for the real and imaginary parts of the potential coincide. The positions of the leading poles were found to be at $r_\pm=(6.58\pm1.65i)$ fm.

III. SEMICLASSICAL CALCULATION OF REGGE POLE POSITIONS AND RESIDUES

The radial Schrödinger equation for the problem is (Ref. [4], p.34)

$$\frac{d^2\psi_l(r)}{dr^2}+\left[\frac{2\mu}{\hbar^2}\left[E-V_N(r)-V_C(r)-\frac{\hbar^2l(l+1)}{2\mu r^2}\right]\right]\times\psi_l(r)=0\ . \tag{3.1}$$

where $V_N(r)$ is the nuclear potential and $V_C(r)$ is the Coulomb potential. The collision energy E is a real parameter but the angular momentum quantum number l is allowed to be complex.

The boundary conditions for a Regge pole are [2,3]

$$\psi(l_n;r=0)=0\ , \tag{3.2}$$

at the origin, and an outgoing-wave-only boundary condition at infinity:

$$\psi(l_n;r)\underset{r\to\infty}{\sim}\exp\{i[kr-\gamma\ln(2kr)]\}\ , \tag{3.3}$$

where l_n is the pole position, $n=0,1,2,\ldots$, and the Sommerfeld parameter γ is $\gamma=e^2Z_1Z_2\mu/\hbar^2k$ with the wave number $k=(2\mu E)^{1/2}/\hbar$. Equation (3.3) differs from the usual boundary condition for a short-range potential by the factor $\exp[-i\gamma\ln(2kr)]$ due to the long-range

TABLE I. Parameters for the four nuclear optical potentials.

Potential	V_0/MeV	r_1/fm	a_1/fm	W_0/MeV	r_2/fm	a_2/fm	r_C/fm
SD	27.456	1.310	0.485	4.865	1.277	0.323	1.0
GK	75.2133	1.2355	0.4929	8.5	1.2065	0.1844	1.4204
E18	10.0	1.35	0.618	23.4	1.23	0.552	1.0
LC	286.5	1.122	3.7	19.7	1.122	0.49	1.2

Coulomb interaction.

The semiclassical procedure for obtaining the pole positions and residues consists in deriving a (uniformly) valid approximation for the wave function in the asymptotic region, and then imposing the outgoing-wave-only boundary condition (3.3) by setting the incoming component of the wave function to zero. This results in an expression for the S matrix element $S(l)$, which yields a semiclassical quantization formula for the pole positions $\{l_n\}$, together with the corresponding residues $\{r_n\}$.

A. Semiclassical wave function

We start our semiclassical analysis by first examining the distribution of classical turning points in the complex r plane. By definition, the classical turning points are solutions of

$$k(l;r)=0 ,$$

where

$$k(l;r)=\left[\frac{2\mu}{\hbar^2}\left[E-V_N(r)-V_C(r)-\frac{\hbar^2(l+\frac{1}{2})^2}{2\mu r^2}\right]\right]^{1/2} ,$$

and the Langer substitution of $(l+\frac{1}{2})^2$ for $l(l+1)$ has also been made.

Figure 1 illustrates the (complex valued) classical turning points closest to the real r axis for $l=0$–50 for the SD potential + uniformly charged sphere interaction at $E_{\rm lab}=55$ MeV ($E=34.994$ MeV). Also illustrated are the positions of the leading poles arising from the Woods-Saxon potential [see Eq. (2.4)]. It can be seen that a_l is always well removed from c_l and e_l but that c_l and e_l can come relatively close to each other.

To obtain the semiclassical wave function for $r\rightarrow\infty$ requires the use of semiclassical formulas. We make two approximations when doing the following. First, we assume linear connection formulas can be used at a_l (which neglects the Coulombic nature of the effective potential close to a_l) together with parabolic connection formulas around c_l and e_l. Secondly, we assume the poles arising from the nuclear potential can be ignored. This is valid provided none of a_l, c_l, e_l lie close to any of these poles. With these assumptions, the semiclassical wave function for $r\rightarrow\infty$ can now be written [from Eq. (12) of Ref. [26]]:

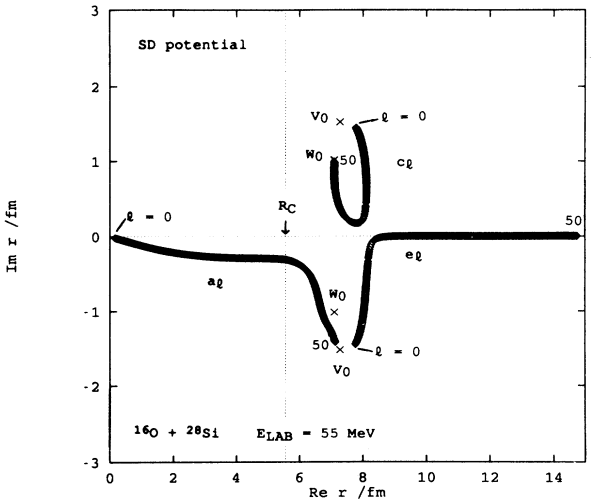

FIG. 1. Turning points a_l,c_l, and e_l for $l=0$–50 in the complex r plane for the SD plus charged sphere potential. R_C denotes the radius of the charged sphere. The locations of the leading potential poles are indicted by crosses, with the poles from the real part of the Woods-Saxon potential labeled V_0, and those from the imaginary part labeled W_0.

$$\psi_l(r)\underset{r\rightarrow\infty}{\sim}[k(l;r)]^{-1/2}(e^{i\alpha}A^-(\epsilon)+e^{-i\alpha}e^{-\pi\epsilon})\exp\left[i\int_{e_l}^{r}k(l;r')dr'-i\frac{1}{4}\pi\right]$$
$$+[k(l;r)]^{-1/2}(e^{-i\alpha}A^+(\epsilon)+e^{i\alpha}e^{-\pi\epsilon})\exp\left[-i\int_{e_l}^{r}k(l;r')dr'+i\frac{1}{4}\pi\right] , \tag{3.4}$$

where $\alpha(l)$ and $\pi\epsilon(l)$ are phase integrals given by

$$\alpha(l)\equiv\int_{a_l}^{c_l}k(l;r)dr \ , \quad \pi\epsilon(l)\equiv -i\int_{c_l}^{e_l}k(l;r)dr \ ,$$

and $A^{\pm}(\epsilon)$ is defined by

$$A^{\pm}(\epsilon)\equiv\frac{(2\pi)^{1/2}}{\Gamma(\frac{1}{2}\mp i\epsilon)}\exp\left[-\frac{1}{2}\pi\epsilon\right]\exp\{\pm i[\epsilon-\epsilon\ln(-\epsilon)]\} .$$

In order to handle potentials with a Coulombic tail, it is convenient to introduce

$$\Delta(l)\equiv\lim_{r\rightarrow\infty}\left[\int_{e_l}^{r}k(l;r')dr'-kr+\gamma\ln(2kr)\right]+\frac{1}{2}\pi\left[l+\frac{1}{2}\right] . \tag{3.5}$$

In terms of $\Delta(l)$, Eq. (3.4) can be written

$$\psi_l(r)\underset{r\rightarrow\infty}{\sim}\exp(-i\tfrac{1}{2}\pi)[k(l;r)]^{-1/2}[e^{i\alpha}A^-(\epsilon)+e^{-i\alpha}e^{-\pi\epsilon}]\exp\{i[kr-\tfrac{1}{2}l\pi-\gamma\ln(2kr)+\Delta(l)]\}$$
$$+\exp(i\tfrac{1}{2}\pi)[k(l;r)]^{-1/2}[e^{-i\alpha}A^+(\epsilon)+e^{i\alpha}e^{-\pi\epsilon}]\exp\{-i[kr-\tfrac{1}{2}l\pi-\gamma\ln(2kr)+\Delta(l)]\} . \tag{3.6}$$

B. Semiclassical S matrix element

The (full) S matrix element, $S(l)$, is defined by

$$\psi_l(r) \underset{r\to\infty}{\sim} N_l(\exp\{-i[kr-\tfrac{1}{2}l\pi-\gamma\ln(2kr)]\} - S(l)\exp\{i[kr-\tfrac{1}{2}l\pi-\gamma\ln(2kr)]\}) , \tag{3.7}$$

where N_l is a normalization constant. Comparison of Eqs. (3.6) and (3.7) shows that the semiclassical S matrix element is given by

$$S(l)=\frac{e^{i\alpha}A^-(\epsilon)+e^{-i\alpha}e^{-\pi\epsilon}}{e^{-i\alpha}A^+(\epsilon)+e^{i\alpha}e^{-\pi\epsilon}}\exp[2i\Delta(l)] . \tag{3.8}$$

This differs from the result for a non-Coulombic potential (see Eq. (19a) of Ref. [26]) by the extra term $\gamma\ln(2kr)$ that is present in the definition of $\Delta(l)$.

The nuclear $S_N(l)$ matrix element is related to $S(l)$ by (Ref. [43], p. 12)

$$S_N(l)=\frac{\Gamma(l+1-i\gamma)}{\Gamma(l+1+i\gamma)}S(l) = e^{-2i\sigma_l}S(l) , \tag{3.9}$$

where σ_l is the Coulomb phase.

C. The phase $\Delta(l)$

It is useful to consider the phase $\Delta(l)$, which is defined by Eq. (3.5), in more detail. After adding and subtracting a term

$$\int_{r_{Cl}}^{r} k_C(l;r')dr' , \tag{3.10}$$

where

$$k_C(l;r)=\left[\frac{2\mu}{\hbar^2}\left[E-\frac{Z_1Z_2e^2}{r}-\frac{\hbar^2(l+\frac{1}{2})^2}{2\mu r^2}\right]\right]^{1/2} = \left[k^2-\frac{2\gamma k}{r}-\frac{(l+\frac{1}{2})^2}{r^2}\right]^{1/2} ,$$

and the classical turning point is given by

$$r_{Cl}=\{\gamma+[\gamma^2+(l+\tfrac{1}{2})^2]^{1/2}\}/k ,$$

we can write $\Delta(l)$ in the form

$$\Delta(l)=\delta_N(l)+\lim_{r\to\infty}\left[\int_{r_{Cl}}^{r}k_C(l;r')dr'-kr+\gamma\ln(2kr)\right] +\frac{1}{2}\pi\left[l+\frac{1}{2}\right] . \tag{3.11}$$

In Eq. (3.11), $\delta_N(l)$ is the nuclear semiclassical phase shift

$$\delta_N(l)\equiv\int_{e_l}^{\infty}k(l;r)dr-\int_{r_{Cl}}^{\infty}k_C(l;r)dr . \tag{3.12}$$

The integral (3.10) can be evaluated explicitly for r large, and we find

$$\lim_{r\to\infty}\int_{r_{Cl}}^{r}k_C(l;r')dr'=kr-\gamma\ln(2kr)-\tfrac{1}{2}\pi(l+\tfrac{1}{2})+\sigma_l^{\mathrm{WKB}} ,$$

where σ_l^{WKB} is the semiclassical (or WKB) approximation to σ_l, namely (Ref. [4], p. 37),

$$\sigma_l^{\mathrm{WKB}}=-\gamma+(l+\tfrac{1}{2})\tan^{-1}[\gamma/(l+\tfrac{1}{2})] +\tfrac{1}{2}\gamma\ln[\gamma^2+(l+\tfrac{1}{2})^2] .$$

Equation (3.11) for $\Delta(l)$ therefore becomes

$$\Delta(l)=\delta_N(l)+\sigma_l^{\mathrm{WKB}} . \tag{3.13}$$

Since $\gamma\gg1$ in our applications to nuclear heavy-ion collisions we can also replace σ_l by σ_l^{WKB} in Eqs. (3.8) and (3.9) for $S_N(l)$, obtaining with the help of Eq. (3.13) the result

$$S_N(l)=\frac{e^{i\alpha}A^-(\epsilon)+e^{-i\alpha}e^{-\pi\epsilon}}{e^{-i\alpha}A^+(\epsilon)+e^{i\alpha}e^{-\pi\epsilon}}\exp[2i\delta_N(l)] . \tag{3.14}$$

D. Semiclassical Regge pole positions and residues

The expression (3.14) for the nuclear S matrix element is formally the same as for non-Coulombic scattering, except that the nuclear phase $\delta_N(l)$ occurs in place of the non-Coulombic WKB phase $\delta(l)$ (see Eq. (19a) of Ref. [26]).

The positions of the Regge poles are obtained by equating the denominator of Eq. (3.14) to zero. This yields the following quantization condition

$$\Phi(l_n)=(n+\tfrac{1}{2})\pi , \quad n=0,1,2,\ldots , \tag{3.15}$$

where

$$\Phi(l)\equiv\alpha(l)-\tfrac{1}{2}\{\epsilon(l)-\epsilon(l)\ln[-\epsilon(l)]\} +\tfrac{1}{2}i\ln\left[\frac{(2\pi)^{1/2}\exp[\frac{1}{2}\pi\epsilon(l)]}{\Gamma(\frac{1}{2}-i\epsilon(l))}\right] , \tag{3.16}$$

and is identical to that for potentials not containing a Coulombic component [26].

The corresponding residues $\{r_n\}$ are obtained by following the procedure in Ref. [26]. We then obtain

$$r_n=i\left[2\frac{d\Phi(l)}{dl}\bigg|_{l=l_n}\right]^{-1}\exp[\pi\epsilon(l_n)-i\alpha(l_n)+i\delta_N(l_n)] , \quad n=0,1,2,\ldots . \tag{3.17}$$

The semiclassical formulas (3.15)–(3.17) involve the three complex turning points a_l,c_l, and e_l and will be referred to as SC(3) in the following.

An important special case arises when c_l and e_l are well separated from each other, so that the phase integral $\epsilon(l)$ is of large modulus. In this case, Stirling's approximation can be applied to the complex gamma function in Eq. (3.16). It is then found that the quantization formula (3.15) simplifies to

$$\omega(l_n)=(n+\tfrac{1}{2})\pi , \quad n=0,1,2,\ldots , \tag{3.18}$$

where

$$\omega(l)=\int_{a_l}^{e_l}k(l;r)dr , \tag{3.19}$$

and is related to α and ϵ by $\omega=\alpha+i\pi\epsilon$. The formula

(3.17) for the residue becomes

$$r_n=-i\left[2\frac{d\omega(l)}{dl}\bigg|_{l=l_n}\right]^{-1}\exp[2i\delta_N(l_n)]\ ,$$

$$n=0,1,2,\ldots\ . \qquad (3.20)$$

Equations (3.18)–(3.20) no longer depend on c_l, and could have been obtained directly by application of linear connection formulas at a_l and e_l. The two-turning-point semiclassical approximations (3.18)–(3.20) will be called SC(2) in the following.

Equations (3.14)–(3.20) are first-order semiclassical approximations. It is likely they can be generalized to arbitrary order, since this has been achieved in the case of non-Coulombic scattering [29,30].

E. Comparison with other results

Restricting l to *real values,* we can compare Eq. (3.14) for $S_N(l)$ with the formula obtained by Brink and Takigawa [43]. If we write

$$e^{\pi\epsilon}A^{+}(\epsilon)=N(-i\epsilon)$$

and

$$e^{\pi\epsilon}A^{-}(\epsilon)=\bar{N}(-i\epsilon)\ ,$$

where

$$N(z)=\frac{(2\pi)^{1/2}}{\Gamma(\frac{1}{2}+z)}\exp[z\ln(z/e)]$$

and

$$\bar{N}(z)=\frac{(2\pi)^{1/2}}{\Gamma(\frac{1}{2}-z)}\exp[i\pi z-z\ln(z/e)]\ ,$$

then Eq. (3.14) can be written in the form

$$S_N(l)=\left[\frac{1+\bar{N}(-i\epsilon)e^{2i\alpha}}{N(-i\epsilon)+e^{2i\alpha}}\right]\exp[2i\delta_N(l)]\ . \qquad (3.21)$$

Equation (3.21) is equivalent to Eq. (2.10) of Ref. [43]. If we set $V_C(r)\equiv 0$, then Eq. (3.14) becomes equivalent to the first-order phase integral formula of Amaha *et al.* [30].

A more general three-turning-point formula for $S(l)$ with l real has been derived by Crowley [44], which takes into account the Coulomb component of the effective potential close to the inner turning point a_l. Equation (3.8) can be obtained from Eq. (3.68) of Ref. [44] as a special case, by setting (in Crowley's notation) $\tilde{\eta}=\eta$ and $\gamma_C=\gamma_C^{\mathrm{WKB}}$.

IV. QUANTUM AND SEMICLASSICAL COMPUTATIONAL METHODS

In this section, we briefly describe the numerical procedures and computer programs used in our calculations for the Regge pole positions and residues.

A. Quantum calculations

The results reported by Takemasa and Tamura (TT) [18] were obtained using the computer code REGGE described by Takemasa, Tamura, and Wolter (TTW) [19]. This computer code is available from the Computer Physics Communications Program Library (catalogue number ABNF) and was employed in our calculations. The TTW code locates the poles and computes the residues of the nuclear S matrix by direct numerical integration of the radial Schrödinger equation. The nuclear S matrix is determined by matching the integrated solution to Coulomb wave functions of complex order [45]. A pole position is then located using a Newton-Raphson iteration in the complex angular momentum plane. In our calculations with the TTW code, the following practical points are important.

(a) The values of the residues are particularly sensitive to numerical factors in the computer codes. In particular, it is important to ensure that the same fundamental constants and conversion factors are used when comparing quantum and semiclassical results. We adjusted the conversion factors in the TTW code so they were consistent with those given by Cohen and Taylor [46]. However, the new conversion factors only differed from the original TTW ones by a few units in the fifth significant figure.

(b) The pole search in the TTW code requires initial estimates for the pole positions and these are either supplied by the user or generated by the program itself.

In order for the program to generate initial estimates of the pole positions in a given region of the complex l plane, the user must manually divide up the specified region into rectangles, whose coordinates are read into the program. The code then evaluates a contour integral around the perimeter of each rectangle; if the modulus of the integral so obtained is $<\delta$, where δ is a small positive number, then the program proceeds to the next rectangle. Otherwise, it searches that rectangle for Regge poles and calculates the residue at each pole. The sum of the residues of the poles in a given rectangle should equal the value obtained by contour integration around the perimeter of the rectangle, thus providing a useful check that no poles have been missed.

It is evident that the program will not find poles with residues that satisfy $|r_n|<\delta$. The default value in the TTW code is $\delta=10^{-3}$ and this value was used by TT. However, we will show in Sec. V that there are poles with $|r_n|<10^{-3}$, and these were therefore missed by TT. To locate these poles, small rectangles and a small integration step length should be chosen, but this greatly increases the expense of the calculation. The program runs much faster if good initial estimates can be supplied, for example, from a semiclassical calculation.

(c) We also examined the stability of the computed pole positions and residues to the number of points used to integrate the radial Schrödinger equation. These are controlled by the integer variables NRMIN and NRMAX. In particular, we systematically varied NRMIN and NRMAX in the ranges 40–80 and 700–1000, respectively. This showed that some of the results reported by TT

are not stable with respect to variations in the number of integration points. In some extreme cases, we were unable to reproduce TT's results with the TTW code.

(d) The TTW code has also been used to calculate Regge poles and residues by Anni and Taffara [20] who describe some modifications to it. They also state (p. 78), "To save computing time we have not verified the stability of all the poles calculated with respect to variation of the number of the integration points of the radial equation. We, in fact, limited ourselves to carrying out some of these checks only at some energies and only for the poles which significantly contribute to the cross section."

(e) The TTW source code as supplied by the Computer Physics Communications Program Library will crash on certain computer systems because it attempts to use variables before they have been initialized. In particular, the complex array UL (used to store the propagating wave function) in subroutine INTE contains uninitialized array elements. This problem can be avoided by filling UL with zeros at the start of the calculation.

B. Semiclassical calculations

The semiclassical computations were carried out using numerical techniques described earlier [26]. Briefly, an initial guess for a pole position l_n is made, which allows the clasical turning points a_{l_n}, c_{l_n}, and e_{l_n} to be evaluated in the complex r plane by Newton-Raphson iteration. The action integrals α, $\pi\epsilon$, and ω are next evaluated by Gaussian integration along straight line segments connecting the turning points. Finally, the initial guess for l_n is improved by Newton-Raphson iteration in the complex l plane. The corresponding residue is then calculated directly using Eqs. (3.17) or (3.20), with the infinite integrals in $\delta_N(l_n)$ truncated at a large finite value.

The procedure just described requires the analytic continuation of the effective potential into the complex r plane. This is straightforward for $V_N(r)$, the centrifugal potential and for a pure Coulomb potential. For the charged sphere potential, we used the following prescription

$$V_C(r)=\begin{cases}\dfrac{e^2Z_1Z_2}{r}\ , & \mathrm{Re}r>R_C\ ,\\ \dfrac{e^2Z_1Z_2}{2R_C}[3-(r/R_C)^2]\ , & \mathrm{Re}r\le R_C\ .\end{cases} \tag{4.1}$$

A difficulty arises in the Gaussian integration when the real parts of the turning points lie on opposite sides of R_C, because there is then a discontinuity in the integrand on the straight line path connecting the turning points. To avoid this difficulty, we used paths of the type

$$a_l\rightarrow(\mathrm{Re}a_l,0)\rightarrow(\mathrm{Re}c_l,0)\rightarrow c_l$$

along which the integrand is free from discontinuities.

In both the quantum and semiclassical calculations the masses used were $m(^{16}\mathrm{O})=15.994$ u and $m(^{28}\mathrm{Si})=27.977$ u. In all cases, $E_{\mathrm{lab}}=55$ MeV, corresponding to a center-of-mass collision energy of $E=34.994$ MeV.

V. RESULTS AND DISCUSSION

Tables II–V contain the Regge pole positions and residues for the SD, E18, GK, and LC potentials, respectively. The abbreviations used in these tables are TT are the quantum results of Takemasa and Tamura as reported in Tables II–V of Ref. [18]; Q are the quantum results obtained using the code REGGE of Takemasa, Tamura, and Wolter (TTW) [19], as described in Sec. IV; SC(2) and SC(3) are the semiclassical two and three turning point results. Usually the SC pole positions and residues are calculated using the two-turning-point formulas (3.18) and (3.20), except when the turning points c_l and e_l are propinquous, in which case the three-turning-point formulas (3.15) and (3.17) are employed. The label n in the tables is the quantum number from the SC quantization formula [Eqs. (3.15) or (3.18)]. As explained below, this number sometimes differs from the label used by TT.

Note that Anni, Renna, and Taffara [47] and Anni and Renna [48] have used TT's pole positions and residues to discuss the angular scattering of ^{16}O colliding with ^{28}Si.

A. Comparison of TT and Q results

TT claim to have located all Regge poles lying in the rectangle $-0.5\le\mathrm{Re}l_n\lesssim 44.5$ and $0\le\mathrm{Im}l_n\lesssim 7$ for all four potentials. However, inspection of our tables shows that they missed the following ten poles: SD($n=7$), GK($n=0$ and 1), and LC($n=0$–6). We first found these poles using SC techniques and subsequently were able to locate five of them with the REGGE code. The exceptions are LD($n=0$–4) which have residues of modulus $<10^{-8}$.

As explained in Sec. IV, we examined the stability of the Q results to variations in the integration parameters for the radial Schrödinger equation. Where appropriate, estimated uncertainties in the Q pole positons and residues are reported in the tables. In general, the accuracy (i.e., the number of significant figures) of the Q results decreases as n increases, with the pole positions more accurate than the residues. Note that for the LC potential with $n\ge 16$, stability problems prevented us from obtaining values for the Q residues, and for $n=21$, the Q pole position as well.

Next, we compare the TT and Q results for the four potentials. The tables show that there is generally good agreement for low values of n, which deteriorates as n increases, in particular for the residues. Note that some of the Q results are more accurate than the corresponding TT ones. Thus for LC($n=7$), TT report $\mathrm{Im}r_7=-0.001$ (one significant figure), whereas the Q result is $\mathrm{Im}r_7=-0.000\,531$ (three significant figures). In contrast, for GK($n=14$), TT have $\mathrm{Im}r_{14}=221.667$ (six significant figures), while the Q calculations give $\mathrm{Im}r_{14}=200\pm 20$ (one significant figure). As noted above, no stable Q values for the residues of LC($n=16$–21) could be obtained.

The E18 potential has just one pole ($n=0$) within the rectangle searched by TT. We also located the $n=1$ pole, which lies just outside this rectangle, and its position and residue are given in Table III.

TABLE II. Positions and residues of the Regge poles for the SD potential. TT are the quantum results of Takemasa and Tamura as reported in Table III of Ref. [18]. Q are the quantum results obtained using the code REGGE (Ref. [19])–present calculations. SC(3) are the semiclassical three-turning-point results using Eqs. (3.15) and (3.17). SC(2) are the semiclassical two-turning-point results using Eqs. (3.18) and (3.20). The numbers in brackets show the estimated uncertainty in the last digit(s) of the Q results, for example $-2.891\ (\pm 1) \equiv -2.892$ to -2.890.

n	Method	$\mathrm{Re}l_n$	$\mathrm{Im}l_n$	$\mathrm{Re}r_n$	$\mathrm{Im}r_n$
0	TT	24.80	1.17	0.241	0.198
	Q	24.802	1.166	0.241	0.198
	SC(3)	24.683	1.172	0.219	0.201
	SC(2)	24.945	0.716	0.0981	0.451
1	TT	22.55	2.27	1.135	1.353
	Q	22.554	2.272	1.135	1.353
	SC(3)	22.449	2.289	1.102	1.380
	SC(2)	22.492	2.322	0.910	1.320
2	TT	19.11	4.05	2.216	−1.732
	Q	19.117	4.051	2.217	−1.732
	SC(3)	19.022	4.052	2.277	−1.517
	SC(2)	19.022	4.052	2.277	−1.517
3	TT	15.08	5.10	−2.891	−0.092
	Q	15.084	5.096	−2.891(±1)	−0.093(±1)
	SC(3)	15.007	5.103	−2.821	−0.258
	SC(2)	15.007	5.103	−2.821	−0.258
4	TT	11.13	5.44	4.067	1.250
	Q	11.134	5.440	4.04(±1)	1.22(±1)
	SC(2)	11.204	5.406	3.709	0.972
5	TT	7.51	5.36	−7.026	−9.934
	Q	7.507(±1)	5.359	−7.02(±2)	−9.96(±2)
	SC(2)	7.852	5.313	−7.512	−4.831
6	TT	4.38	4.89	−35.358	24.621
	Q	4.380	4.896	−35.44(±1)	24.54(±2)
	SC(2)	4.921	5.030	1.967	33.53
7	TT				
	Q	1.823(±1)	4.370(±1)	−25.3(±2)	143.8(±3)
	SC(2)	2.351	4.659	157.9	39.84
8	TT[a]	−0.36	3.89	−55.732	369.174
	Q	−0.37(±1)	3.90(±1)	−62(±15)	395(±30)
	SC(2)	0.0842	4.264	703.3	0.378

[a]Assigned to $n = 7$ by TT in Table III of Ref. [18].

TABLE III. Positions and residues of the Regge poles for the E18 potential. Notation same as Table II. The TT result is from Table II of Ref. [18].

n	Method	$\mathrm{Re}l_n$	$\mathrm{Im}l_n$	$\mathrm{Re}r_n$	$\mathrm{Im}r_n$
0	TT	23.79	4.20	1.773	0.667
	Q	23.789	4.200	1.773	0.667
	SC(2)	23.752	4.290	1.594	0.653
1	TT				
	Q	22.612	8.272	0.72(±2)	−0.68(±3)
	SC(2)	22.611	8.386	0.744	−0.627

TABLE IV. Positions and residues of the Regge poles for the GK potential. Notation is the same as Table II. The TT results are from Table IV of Ref. [18].

n	Method	Rel_n	Iml_n	Rer_n	Imr_n
0	TT				
	Q	34.233	1.886	-0.114×10^{-7}	$-0.943(\pm1)\times10^{-8}$
	SC(3)	34.178	1.880	-0.111×10^{-7}	-0.917×10^{-8}
1	TT				
	Q	31.159	1.645(±1)	-0.127×10^{-5}	-0.133×10^{-4}
	SC(3)	31.126	1.619	0.191×10^{-6}	-0.136×10^{-4}
2	TT[a]	28.39	1.46	0.2×10^{-2}	-0.2×10^{-2}
	Q	28.395	1.462	0.161×10^{-2}	-0.192×10^{-2}
	SC(3)	28.371	1.481	0.165×10^{-2}	-0.181×10^{-2}
3	TT[a]	26.00	1.29	0.125	0.029
	Q	26.005	1.287	0.125	0.0289
	SC(3)	25.957	1.303	0.128	0.0298
4	TT[a]	24.17	1.58	0.312	0.739
	Q	24.171	1.580	0.312	0.739
	SC(3)	24.138	1.582	0.288	0.765
	SC(2)	24.265	1.615	0.0549	0.724
5	TT[a]	21.94	2.39	1.089	1.234
	Q	21.940	2.394	1.088	1.234
	SC(2)	21.925	2.416	0.927	1.277
6	TT[a]	19.41	3.06	2.691	−0.606
	Q	19.412	3.065	2.692	−0.604
	SC(2)	19.392	3.079	2.702	−0.424
7	TT[a]	16.78	3.56	−0.444	−4.021
	Q	16.785	3.563	−0.439	−4.022
	SC(2)	16.790	3.569	−0.370	−3.960
8	TT[a]	14.13	3.90	−5.599	1.272
	Q	14.132	3.902	−5.603	1.262
	SC(2)	14.204	3.895	−5.147	1.754
9	TT[a]	11.48	4.07	3.024	7.524
	Q	11.486	4.073	3.012(±3)	7.532(±2)
	SC(2)	11.683	4.090	5.189	5.773
10	TT[a]	8.94	4.07	9.466	−5.858
	Q	8.942	4.067	9.47(±1)	−5.84(±1)
	SC(2)	9.279	4.127	3.915	−10.47
11	TT[a]	6.55	3.98	−11.140	−13.363
	Q	6.558	3.978	−11.056(±2)	−13.37(±1)
	SC(2)	6.934	4.161	−21.69	−0.931
12	TT[a]	4.31	3.87	−28.013	18.972
	Q	4.303(±1)	3.867(±2)	−28.31(±5)	18.8(±1)
	SC(2)	4.671	4.141	−0.838	52.42
13	TT[a]	2.14	3.74	0.436	81.375
	Q	2.14(±1)	3.755(±5)	2.6(±5)	83(±2)
	SC(2)	2.486	4.081	140.4	70.60
14	TT[a]	0.02	3.62	60.961	221.667
	Q	0.07(±1)	3.65(±3)	100(±20)	200(±20)
	SC(2)	0.372	3.992	530.2	5.547

[a]The entries for $n=2-14$ are assigned to $n=0-12$ by TT in Table IV of Ref. [18].

TABLE V. Positions and residues of the Regge poles for the LC potential. Notation is the same as Table II. The TT results are from Table V of Ref. [18].

n	Method	$\mathrm{Re}l_n$	$\mathrm{Im}l_n$	$\mathrm{Re}r_n$	$\mathrm{Im}r_n$
0	SC(3)	44.925	1.522	-0.105×10^{-19}	-0.160×10^{-19}
1	SC(3)	42.312	1.518	-0.233×10^{-16}	-0.618×10^{-16}
2	SC(3)	39.819	1.510	-0.870×10^{-14}	-0.646×10^{-13}
3	SC(3)	37.430	1.499	0.270×10^{-11}	-0.266×10^{-10}
4	SC(3)	35.134	1.485	0.181×10^{-8}	-0.505×10^{-8}
5	TT				
	Q	32.939	1.465	$0.314(\pm1)\times10^{-6}$	$-0.479(\pm1)\times10^{-6}$
	SC(3)	32.921	1.466	0.327×10^{-6}	-0.481×10^{-6}
6	TT				
	Q	30.806	1.441	0.268×10^{-4}	-0.236×10^{-4}
	SC(3)	30.787	1.442	0.279×10^{-4}	-0.235×10^{-4}
7	TT[a]	28.75	1.41	0.1×10^{-2}	-0.1×10^{-2}
	Q	28.754	1.406	0.125×10^{-2}	-0.531×10^{-3}
	SC(3)	28.735	1.407	0.130×10^{-2}	-0.518×10^{-3}
8	TT[a]	26.81	1.34	0.032	0.4×10^{-2}
	Q	26.815	1.340	0.0324	0.367×10^{-2}
	SC(3)	26.796	1.340	0.0330	0.494×10^{-2}
9	TT[a]	25.14	1.33	0.167	0.258
	Q	25.142	1.331	0.167	0.257
	SC(3)	25.125	1.334	0.158	0.267
10	TT[a]	23.50	1.72	0.175	0.840
	Q	23.505	1.722	0.175	0.839
	SC(3)	23.466	1.674	0.144	0.867
	SC(2)	23.537	1.747	0.726×10^{-2}	0.795
11	TT[a]	21.60	2.21	0.992	1.277
	Q	21.602	2.206	0.990	1.278
	SC(3)	21.598	2.219	0.838	1.328
	SC(2)	21.598	2.219	0.838	1.328
12	TT[a]	19.57	2.632	2.748	0.044
	Q	19.575(±1)	2.632	2.748	0.048(±1)
	SC(2)	19.564	2.640	2.709	0.261
13	TT[a]	17.48	2.99	1.629	−3.869
	Q	17.487(±1)	2.993(±2)	1.63(±1)	−3.85(±2)
	SC(2)	17.473	3.001	1.891	−3.731
14	TT[a]	15.36	3.30	−5.177	−3.102
	Q	15.36(±1)	3.30(±1)	−5.10(±15)	−3.2(±1)
	SC(2)	15.350	3.300	−4.879	−3.396
15	TT[a]	13.29	3.54	−3.129	7.127
	Q	13.26(±10)	3.6(±1)	−3.8(±12)	7.6(±6)
	SC(2)	13.215	3.539	−4.425	6.906
16	TT[a]	11.17	3.41	6.077	2.780
	Q	10.9(±12)	3.6(±2)	b	b
	SC(2)	11.083	3.724	10.60	4.735

TABLE V. (*Continued*).

n	Method	Rel_n	Iml_n	Rer_n	Imr_n
17	TT[a]	8.56	3.44	5.276	−3.309
	Q	7.9(±11)	3.3(±5)	b	b
	SC(2)	8.960	3.861	4.232	−17.31
18	TT[a]	6.57	2.64	−0.653	−2.154
	Q	5.7(±8)	3.0(±8)	b	b
	SC(2)	6.852	3.957	−31.19	−4.011
19	TT[a]	3.74	2.07	0.064	−0.901
	Q	2.9(±9)	2.2(±4)	b	b
	SC(2)	4.760	4.016	−14.16	65.77
20	TT[a]	1.27	1.80	0.314	−0.627
	Q	0.9(±4)	1.8(±2)	b	b
	SC(2)	2.687	4.058	142.7	110.2
21	TT				
	Q	c	c	c	c
	SC(2)	0.631	4.049	577.6	52.53

[a]The entries for $n=7-20$ are assigned to $n=0-13$ by TT in Table V of Ref. [18].
[b]The uncertainties in Rel_n and Iml_n are too large to allow approximate estimates for Rer_n and Imr_n to be made.
[c]The uncertainties in Rel_{21} and Iml_{21} are too large to allow approximate estimates for these quantities, and hence also for Rer_{21} and Imr_{21}.

B. Comparison of Q and SC results

TT labeled the poles $n=0,1,2,\ldots$, according to the decreasing value of the real part of the pole position. Table II–V show this procedure is in one-to-one correspondence with the SC quantum number n. Thus if TT had not missed ten poles, their labeling scheme would have agreed with the SC one.

Table II shows that the Q and SC(3) pole positions for the SD potential for $n=0-3$ agree to better than 1%, with the SC(3) residues being less accurate. Also note the improvement for $n=0$ of the SC(3) results compared to SC(2). As n increases, the accuracy of the SC(2) results gradually decreases, particularly for $n \geq 6$.

This decrease in accuracy can be understood by examining the positions of the turning points a_{l_n}, c_{l_n}, and e_{l_n} in the complex r plane. They are plotted in Fig. 2, which reveals that c_{l_n} and e_{l_n} migrate, as n increases, towards the leading poles of the real part of the SD potential. Since the SC connection formulas we have used in Sec. II are not valid close to poles of the potential, this provides a possible reason for the decrease in accuracy of the SC results with increasing n. Notice also that, unlike Fig. 1, e_{l_n} lies in the first quadrant and c_{l_n} lies in the fourth quadrant of the complex r plane. The turning points for the E18 potential shown in Fig. 3 are well removed from each other and from the potential poles and, as expected, the SC(2) and Q results in Table III are in good agreement.

The SC results for the GK and LC potentials in Tables IV and V, respectively, follow a similar trend to those for the SD potential in Table II. Examination of the turning-point trajectories for the GK potential in Fig. 4 and for the LC potential in Fig. 5 again shows c_{l_n} and e_{l_n} migrating towards the leading potential poles with increasing n, thereby explaining the decrease in accuracy of the SC results.

The turning points in Figs. 2–5 were obtained as follows. The SC(3) pole positions were used to calculate a_{l_n}, c_{l_n}, and e_{l_n} directly for those cases in Tables II–V which report SC(3) results. For the remaining cases, the SC(2) pole positions were employed to obtain a_{l_n} and e_{l_n}, and then c_{l_n} was calculated.

An important advantage of the SC method for the LC potential is that it finds the $n=0-4$ poles, whose residues are too small in magnitude ($<10^{-8}$) for the REGGE code to detect. Similarly for the $n=0$ and 1 poles of the GK potential, the SC results provide initial estimates for the REGGE code, which would have difficulties otherwise in locating them (these poles were missed by TT).

Inspection of Figs. 2–5 shows that the real parts of the turning points sometimes lie on opposite sides of R_C, the Coulomb radius for the charged sphere potential (2.3). For these cases, the charged sphere potential has been analytically continued according to the reasonable (but nevertheless arbitrary) prescription (4.1). We also used paths along which the action integrals are continuous, as described in Sec. IV B. The good agreement between the Q and SC results in the tables (for cases where the turning points are not close to the potential poles) indicates that the WKB theory of Sec. II is accurate under conditions less restrictive than those commonly assumed. The usual assumption is that the effective potential is analytic in r (apart from possible poles) in a region close to the Rer

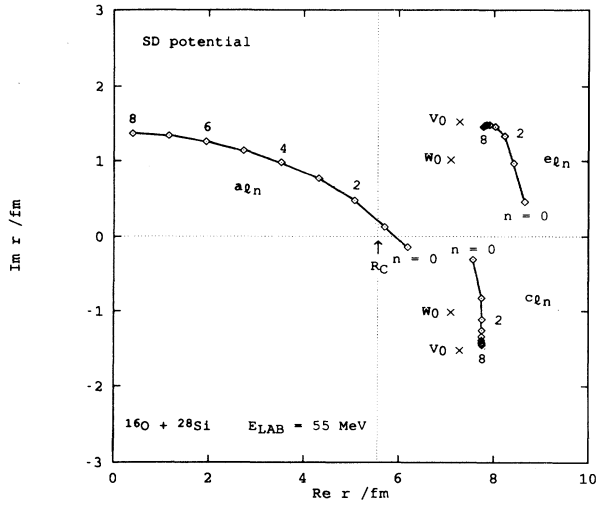

FIG. 2. Turning points a_{l_n}, c_{l_n}, and e_{l_n} for $n=0$–8 in the complex r plane for the SD plus charged sphere potential. Turning points with different values of n have been joined by straight lines. R_C denotes the radius of the charged sphere. The locations of the leading potential poles are indicated by crosses, with the poles from the real part of the Woods-Saxon potential labeled V_0, and those from the imaginary part labeled W_0.

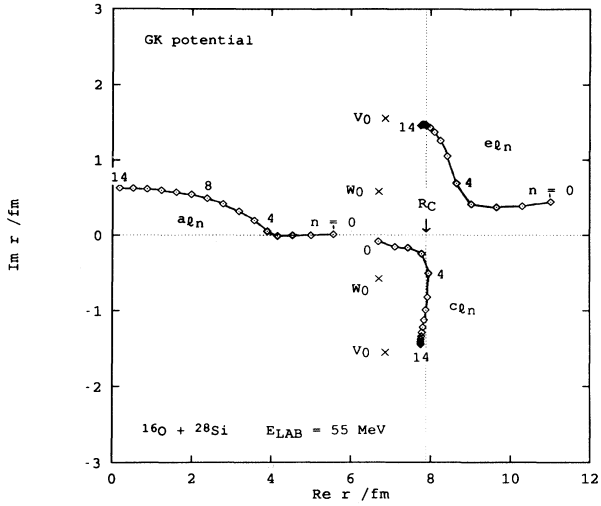

FIG. 4. Same as Fig. 2, except for the GK plus charged sphere potential and $n=0$–14.

axis. For example, Brink and Takigawa modified the charged sphere potential so that it is analytic for all $r\neq 0$ (Eqs. (4.1) and (4.2) of Ref. [43]). It would be interesting to repeat the SC calculations of Refs. [43,48,49] using the prescription Eq. (4.1). Delos and Carlson [25] and Thylwe [31] have also done WKB calculations with a piecewise continuous potential.

For the LC potential, Shastry and Parija [8] have compared the poles obtained from $N(-i\epsilon)=0$ in Eq. (3.21) with the TT pole positions. The agreement between the two sets of results is poor. However, this is not surprising because $N(-i\epsilon)=0$ does not determine the poles of $S_N(l)$, and the analytic structure of $N(-i\epsilon)$ and $S_N(l)$ are different [8,48,50].

It is expected that the position of the leading pole from $N(-i\epsilon)=0$ correlates with the Regge pole closest to the Rel axis [8,48]. This leading pole is located at (24.436, 1.954) for SD [48], (23.77, 4.28) [48] or (23.73, 4.26) [47] for E18, (25.363, 2.142) for GK [48], and (25.02, 0.187) for LC [8]. These values are to be compared with the Q pole positions of $l_0=(24.802, 1.166)$ for SD, $l_0=(23.789, 4.200)$ for E18, $l_3=(26.005, 1.287)$ for GK, and $l_9=(25.142, 1.331)$ for LC. It is evident that the error for the imaginary part of the leading pole position from $N(-i\epsilon)=0$ is much larger than that for the real part.

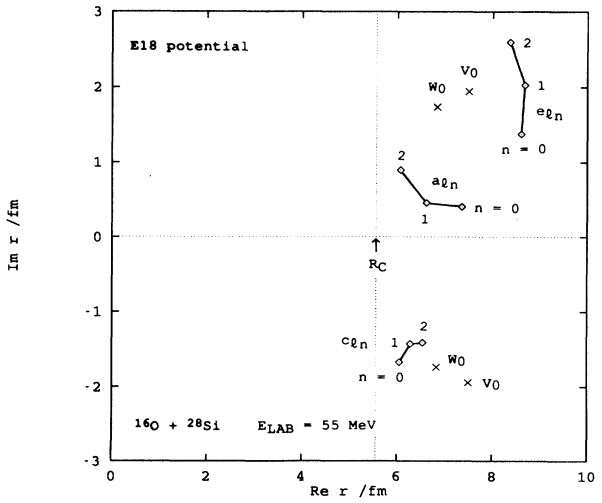

FIG. 3. Same as Fig. 2, except for the E18 plus charged sphere potential and $n=0$–2.

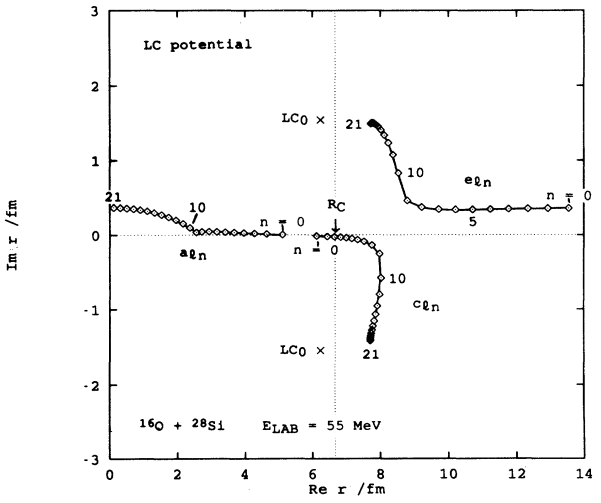

FIG. 5. Same as Fig. 2, except for the LC plus charged sphere potential and $n=0$–21. The leading potential poles are labeled LC_0.

C. Pure Coulomb potential

The results discussed in Secs. V A and V B have all employed the charged sphere potential (2.3) and its analytic continuation, Eq. (4.1). We have examined the effect of using a pure Coulomb potential for all r

$$V_C(r)=e^2Z_1Z_2/r\ , \tag{5.1}$$

by calculating SC(2) and SC(3) pole positions and residues for the SD and GK potentials. These results are reported in Table VI.

When the real parts of all three turning points are

TABLE VI. Semiclassical results for the positions and residues of the Regge poles for the SD and GK potentials plus a pure Coulomb interaction.

n	Method	Rel_n	Iml_n	Rer_n	Imr_n
		SD potential (+ pure Coulomb interaction)			
0	SC(3)	24.683	1.172	0.219	0.201
	SC(2)	24.945	0.716	0.0981	0.451
1	SC(3)	22.449	2.289	1.102	1.380
	SC(2)	22.492	2.322	0.910	1.320
2	SC(2)	19.069	4.096	2.152	−1.536
3	SC(2)	15.072	5.539	−2.152	0.136
4	SC(2)	11.029	6.668	1.368	−0.585
5	SC(2)	7.276	7.844	−0.290	1.165
6	SC(2)	4.149	9.169	−1.094	−0.741
7	SC(2)	1.721	10.313	1.775	−2.164
8	SC(2)	−0.311	11.099	12.09	−2.746
		GK potential (+ pure Coulomb interaction)			
0	SC(3)	33.674	1.882	-0.352×10^{-7}	-0.304×10^{-7}
1	SC(3)	30.486	1.614	0.521×10^{-5}	-0.506×10^{-4}
2	SC(3)	27.583	1.469	0.827×10^{-2}	-0.633×10^{-2}
3	SC(3)	25.228	1.311	0.277	0.237
	SC(2)	25.281	0.652	0.0421	0.311
4	SC(3)	23.210	2.102	0.569	1.149
	SC(2)	23.260	2.141	0.401	1.074
5	SC(2)	20.538	3.189	2.155	0.429
6	SC(2)	17.537	4.137	0.346	−2.905
7	SC(2)	14.381	4.951	−2.637	1.552
8	SC(2)	11.172	5.689	3.016	−0.307
9	SC(2)	8.002	6.478	−3.374	0.139
10	SC(2)	5.046	7.433	4.855	−1.028
11	SC(2)	2.527	8.449	−11.83	5.502
12	SC(2)	0.406	9.275	98.75	−97.11
13	SC(2)	−1.507	9.852	8.860×10^{3}	-9.109×10^{4}

greater than R_C, the potentials (4.1) and (5.1) are identical as far as the SC theory is concerned. This ocurs for SD($n=0$ and 1). Comparing Tables II and IV with Table VI shows that the pole positions using the charged sphere potential increasingly diverge from the pure Coulomb positions as $\mathrm{Re}a_{l_n}$ moves within R_C. In particular, for large n, $\mathrm{Im}l_n$ increases monotonically for the pure Coulomb potential, whereas the poles for the charged sphere potential start to bend back toward the Rel axis. There are corresponding changes in the residues.

Using a pure Coulomb potential, Knoll and Schaeffer [22] have calculated three SC(2) pole positions ($n=0$, 1, and 2) at three energies in order to compare with quantum results of Tamura and Wolter [17]. The SC(2) pole positions agree well with the quantum ones (see Table II of Ref. [22]). Knoll and Schaeffer also state (Ref. [22], p. 320, footnote 5): "For simplicity reasons we have taken a pure Coulomb force even in the interior of the nucleus. This provides us with an analytical expression for $V(r)$. Anyhow, the results are not very sensitive to the interior because of absorption." However, our results in Tables II, IV, and VI show that this last sentence is not true, in general, in particular for large values of n.

VI. CONCLUSIONS

We have reported the first uniform SC calculations of Regge pole positions and residues for complex optical nuclear heavy-ion potentials, by applying (and generalizing) SC techniques originally developed for atomic and molecular scatterings. We used the SD, GK, E18, and LC potentials, which have been fitted to $^{16}O+^{28}Si$ elastic-scattering data. Our SC computations revealed that TT had missed ten poles. Using a modified version of the REGGE code, we were able to locate five of these poles. We also found that some of the results reported by TT are unstable with respect to variations in the number of integration points for the radial Schrödinger equation.

For low values of n, the SC and Q pole positions are in close agreement, with larger differences for the residues—this same behavior is found in the atomic and molecular case [25–34]. However, as n increases, the SC results became less accurate. This loss of accuracy probably arises because the outer turning points migrate towards the leading poles of the nuclear potential with increasing n, an effect ignored in the SC analysis.

An advantage of the SC method is the unique assignment of quantum numbers to Regge poles; this labeling ensures that no poles are missed. We also demonstrated that the choice for $V_C(r)$—charged sphere or pure Coulomb—can have a significant effect on the propeties of the Regge pole positions and residues.

Our investigation suggests several topics for future research:

(a) The Q pole positions and residues in Tables II–V are the *best available* quantum results for heavy-ion potentials at the present time. However, the instability problems in the REGGE code, discussed in Sec. IV, limit the accuracy of the poles as n increases, as well as for small n when the residues are very small in magnitude. It is clearly desirable to discover new numerical algorithms to overcome these problems.

(b) The SC theory should be extended to allow for the uniform coalescence of a turning point with a pole of the nuclear potential.

(c) The SC calculations used a piecewise analytic potential. We found the results remained accurate under conditions less restrictive than those commonly assumed in a WKB treatment. It would be interesting to investigate this finding in more detail.

ACKNOWLEDGMENTS

We thank Dr. K.-E. Thylwe, Department of Mechanics, Royal Institute of Technology, Stockholm, Sweden for useful discussions. Support of this research by the U.K. Science and Engineering Research Council is gratefully acknowledged.

[1] H. M. Nussenzveig, *Diffraction Effects in Semiclassical Scattering* (Cambridge University Press, Cambridge, England, 1992).

[2] R. G. Newton, *The Complex j Plane* (Benjamin, New York, 1964).

[3] V. de Alfaro and T. Regge, *Potential Scattering* (North-Holland, Amsterdam, 1965).

[4] D. M. Brink, *Semiclassical Methods for Nucleus-Nucleus Scattering* (Cambridge University Press, Cambridge, England, 1985).

[5] M. S. Child, *Semiclassical Mechanics with Molecular Applications* (Clarendon Press, Oxford, England, 1991).

[6] K. W. McVoy, Phys. Rev. C **3**, 1104 (1971); in *Classical and Quantum Mechanical Aspects of Heavy Ion Collisions,* Vol. 33 of *Lecture Notes in Physics,* edited by H. L. Harney, P. Braun-Munzinger, and C. K. Gelbke (Springer, Berlin, 1975), pp. 127–139; B. V. Carlson and K. W. McVoy, Nucl. Phys. **A292**, 310 (1977); K. W. McVoy, Notas **1**(4) (1978).

[7] R. C. Fuller, Nucl. Phys. **A216**, 199 (1973); R. C. Fuller and Y. Avishai, *ibid.* **A222**, 365 (1974); R. C. Fuller and O. Dragun, Phys. Rev. Lett. **32**, 617 (1974); R. C. Fuller and K. W. McVoy, Phys. Lett. **55B**, 121 (1975); R. C. Fuller and P. J. Moffa, Phys. Rev. C **14**, 1721 (1976); **15**, 266 (1977); R. C. Fuller, *ibid.* **16**, 1865 (1977).

[8] C. S. Shastry and I. Parija, Phys. Rev. C **27**, 2042 (1983).

[9] M. El-Nadi and A. Osman, Ann. Phys. (Leipzig) **33**, 341 (1976); A. Y. Abul-Magd, H. M. Khalil, and M. M. Shalaby, J. Phys. G **3**, 381 (1977); M. M. Shalaby and H. M. Khalil, *ibid.* **4**, L293 (1978); M. M. Shalaby, A. M. El Naiem, H. M. Khalil, and M. A. Ali, Acta Phys. Acad. Scient. Hung. **50**, 3 (1981); C. S. Shastry and R. K. Satpathy, Proc. Indian Nat. Sci. Acad. A **47**, 373 (1981).

[10] I. M. Brâncuş, Stud. Cercet. Fiz. **33**, 565 (1981); I. M. Brâncuş, A. Constantinescu, I. Lazăr, I. Mihai, M. Petraşcu, A. S. Demianova, A. A. Ogloblin, and S. B. Sakuta, Rev. Roum. Phys. **29**, 77 (1984).

[11] N. Rowley and C. Marty, Phys. Lett. **55B**, 430 (1975);

Nucl. Phys. **A266**, 494 (1976).
[12] M. C. Mermaz, Phys. Rev. C **24**, 773 (1981); M. C. Mermaz, E. R. Chavez-Lomeli, J. Barrette, B. Berthier, and A. Greiner, *ibid.* **29**, 147 (1984).
[13] P. Braun-Munzinger, G. M. Berkowitz, T. M. Cormier, C. M. Jachcinski, J. W. Harris, J. Barrette, and M. J. LeVine, Phys. Rev. Lett. **38**, 944 (1977); P. Braun-Munzinger and J. Barrette, Phys. Rep. **87**, 209 (1982).
[14] N. Takigawa and S. Y. Lee, Nucl. Phys. **A292**, 173 (1977); S. Y. Lee, N. Takigawa, and C. Marty, *ibid.* **A308**, 161 (1978).
[15] R. Anni, L. Renna, and L. Taffara, Nuovo Cimento A **55**, 456 (1980); **59**, 38 (1980); E. Di Salvo, *ibid.* **74**, 427 (1983); J. P. F. Sellschop, A. Zucchiatti, L. Mirman, M. Z. I. Gering, and E. Di Salvo, J. Phys. G **13**, 1129 (1987).
[16] K. A. Gridnev and A. A. Ogloblin, Fiz. Elem. Chastits At. Yadra **6**, 393 (1975) [Sov. J. Part. Nucl. **6**, 158 (1975)]; K. M. Hartmann, Z. Phys. A **282**, 293 (1977); S. Landowne, Phys. Rev. Lett. **42**, 633 (1979); B. Huang, Y. Wang, R. Yuan, J. Yuan, S. Li, X. Bao, and Z. Sun, Chin. J. Nucl. Phys. **6**, 156 (1984) [Chin. Phys. **5**, 420 (1985)]; S. G. Cooper, M. W. Kermode, and L. J. Allen, J. Phys. G **12**, L291 (1986); S. Yu. Kun, M. Papa, and D. K Sunko, Phys. Lett. B **249**, 1 (1990).
[17] T. Tamura and H. H. Wolter, Phys. Rev. C **6**, 1976 (1972).
[18] T. Takemasa and T. Tamura, Phys. Rev. C **18**, 1282 (1978).
[19] T. Takemasa, T. Tamura, and H. H. Wolter, Comput. Phys. Commun. **18**, 427 (1979).
[20] R. Anni and L. Taffara, Nuovo Cimento A **79**, 159 (1984); K. M. Khalil, K. W. McVoy, and M. M. Shalaby, Nucl. Phys. **A455**, 100 (1986).
[21] H. M. Khalil, M. M. Shalaby, and M. A. El-Keriem, Fizika **17**, 465 (1985).
[22] J. Knoll and R. Schaeffer, Ann. Phys. (N.Y.) **97**, 307 (1976).
[23] E. A. Remler, Phys. Rev. A **3**, 1949 (1971); S. M. Bobbio, W. G. Rich, L. D. Doverspike, and R. L. Champion, *ibid.* **4**, 957 (1971); W. G. Rich, S. M. Bobbio, R. L. Champion, and L. D. Doverspike, *ibid.* **4**, 2253 (1971); L. D. Doverspike, in *The Physics of Electronic and Atomic Collisions, Invited Lectures and Progress Reports,* VIIIth ICPEAC, edited by B. C. Čorbić and M. V. Kurepa (Institute of Physics, Beograd, Yugoslavia, 1973), pp. 297–309.
[24] J. N. L. Connor, Mol. Phys. **29**, 745 (1975); J. N. L. Connor and W. Jakubetz, Chem. Phys. Lett. **36**, 29 (1975); Mol. Phys. **33**, 1619 (1977); J. N. L. Connor and D. C. Mackay, Chem. Phys. **40**, 11 (1979).
[25] J. B. Delos and C. E. Carlson, Phys. Rev. A **11**, 210 (1975).
[26] J. N. L. Connor, W. Jakubetz, and C. V. Sukumar, J. Phys. B **9**, 1783 (1976).
[27] J. N. L. Connor, J. B. Delos, and C. E. Carlson, Mol. Phys. **31**, 1181 (1976); J. N. L. Connor and W. Jakubetz, *ibid.* **35**, 949 (1978); J. N. L. Connor and D. C. Mackay, Chem. Phys. Lett. **59**, 163 (1978); J. N. L. Connor, D. C. Mackay, and C. V. Sukumar, J. Phys. B **12**, L515 (1979); J. N. L. Connor, W. Jakubetz, D. C. Mackay, and C. V. Sukumar, *ibid.* **13**, 1823 (1980); J. N. L. Connor, D. Farrelly, and D. C. Mackay, J. Chem. Phys. **74**, 3278 (1981); J. N. L. Connor, J. Phys. B **15**, 1683 (1982); K.-E. Thylwe and J. N. L. Connor, J. Phys. A **18**, 2957 (1985); J. N. L. Connor, D. C. MacKay, and K.-E. Thylwe, J. Chem. Phys. **85**, 6368 (1986); J. N. L. Connor and K.-E. Thylwe, *ibid.* **86**, 188 (1987).
[28] K.-E. Thylwe and J. N. L. Connor, J. Phys. B. **21**, L597 (1988); J. Chem. Phys. **91**, 1668 (1989); J. N. L. Connor, P. McCabe, and K.-E. Thylwe, J. Phys. B **24**, 2503 (1991); P. McCabe, J. N. L. Connor, and K.-E. Thylwe, J. Chem. Phys. **98**, 2947 (1993).
[29] N. Fröman and P. O. Fröman, Phys. Rev. A **43**, 3563 (1991); K.-E. Thylwe and A. Amaha, *ibid.* **43**, 3567 (1991); A. Amaha and K.-E. Thylwe, *ibid.* **44**, 4203 (1991).
[30] A. Amaha, A. Dzieciol, N. Fröman, P. O. Fröman, and K.-E. Thylwe, Phys. Rev. A **45**, 1596 (1992). Equation (5.5) should be multiplied by $\exp[2i\delta(l)]$ to be consistent with Eq. (5.1).
[31] K.-E. Thylwe, J. Phys. B **16**, 1915 (1983).
[32] K.-E. Thylwe, J. Phys. A **16**, 1141 (1983); **16**, 3325 (1983); **18**, 3445 (1985).
[33] C. V. Sukumar and J. N. Bardsley, J. Phys. B **8**, 568 (1975); C. V. Sukumar, S. L. Lin, and J. N. Bardsley, *ibid.* **8**, 577 (1975); S. Bosanac and K. Knešaurek, Phys. Rev. A **28**, 2173 (1983); J. Luppi, J. Comput. Phys. **71**, 111 (1987); P. Pajunen, J. Chem. Phys. **88**, 4268 (1988); S. Kais and G. Beltrame, J. Phys. Chem. **97**, 2453 (1993).
[34] N. Andersson (unpublished).
[35] J. N. L. Connor, Chem. Soc. Rev. **5**, 125 (1976).
[36] J. N. L. Connor, in *Semiclassical Methods in Molecular Scattering and Spectroscopy,* Proceedings of the NATO Advanced Study Institute, Cambridge, 1979, edited by M. S. Child (Reidel, Dordrecht, The Netherlands, 1980), pp. 45–107.
[37] J. N. L. Connor, J. Chem. Soc. Faraday Trans. **86**, 1627 (1990).
[38] K.-E. Thylwe, in *Resonances, The Unifying Route Towards the Formulation of Dynamical Processes. Foundations and Applications in Nuclear, Atomic and Molecular Physics,* Vol. 325 of Lecture Notes in Physics, edited by E. Brändas and N. Elander (Springer, Berlin, 1989), pp. 281–311.
[39] Reference 4 of Ref. [18].
[40] Reference 5 of Ref. [18].
[41] J. G. Cramer, R. M. DeVries, D. A. Goldberg, M. S. Zisman, and C. F. Maguire, Phys. Rev. C **14**, 2158 (1976).
[42] Reference 6 and Table I of Ref. [18].
[43] D. M. Brink and N. Takigawa, Nucl. Phys. **A279**, 159 (1977).
[44] B. J. B. Crowley, Phys. Rep. **57**, 47 (1980).
[45] T. Takemasa, T. Tamura, and H. H. Wolter, Comput. Phys. Commun. **17**, 351 (1979).
[46] E. R. Cohen and B. N. Taylor, J. Phys. Chem. Ref. Data **2**, 663 (1973).
[47] R. Anni, L. Renna, and L. Taffara, Lett. Nuovo Cimento **25**, 121 (1979).
[48] R. Anni and L. Renna, Nuovo Cimento A **65**, 311 (1981).
[49] S. Y. Lee, Nucl. Phys. **A311**, 518 (1978); A. R. Farhan, B. J. Stoyanov, A. Nagl, H. Überall, and M. de Llano, Phys. Rev. C **34**, 2134 (1986).
[50] W. A. Friedman and C. J. Goebel, Ann. Phys. (N.Y.) **104**, 145 (1977); I. A. Gubkin, Yad. Fiz. **28**, 654 (1978) [Sov. J. Nucl. Phys. **28**, 336 (1978)].